On generalized differences for Biospeckle image analysis

André V. Saúde*, Fortunato S. de Menezes†, Patrícia L. S. Freitas ‡§, Giovanni F. Rabelo‡ and Roberto A. Braga Jr.‡
*Department of Computer Science
†Department of Exact Science
‡Department of Enginnering
Federal University of Lavras, Campus Universitário
Cx. Postal 3037, Lavras, MG, Brasil
§Graduate and Research Division
UNIFENAS - José do Rosário Vellano University
Email: {saude,fmenezes,rabelo,robbraga}@ufla.br, patricia.freitas@posgrad.ufla.br

***Abstract*—Biospeckle is a technique whose purpose is to observe and study the underlying activity of some material. The technique has its roots on optical physics, and its first step is an image acquisition process that produces a video sequence whose characteristics allow researchers to have an interpretation of the activity of the activity of the observed material by an analysis of the video content. The recent literature on this subject presents several different measurements for analyzing the video sequence. One of the most popular measurement is the Generalized Difference (GD). The computation of the GD has an asymptotic complexity of $\mathcal{O}(n^2)$. In this paper we propose: i) an alternative $\mathcal{O}(n)$ algorithm for the computation of the GD, and ii) an alternative measurement, that we call GD^*. We discuss the qualitative similarities between the GD and the GD^*. We conclude that the GD^* is an alternative generalized difference measurement, and thus it can replace the GD in many applications. We show that the GD^* is a function of the variance, and it can be computed in $\mathcal{O}(n)$. Finally, if the GD itself is desired as measurement, it can now be computed in $\mathcal{O}(n)$ by the novel algorithm presented in this paper.**

***Keywords*-image analysis; optical physics; biospeckle; statistical image analysis;**

I. Introduction

Biospeckle is a technique which has its roots on Physics, mainly optical physics [1], [2], [3]. It does use the interference properties of monochromatic light (usually, laser on a specific range of wavelength) reflected on the object (sample) studied to access its activity. Although the light is monochromatic, its reflection on the object (sample) produces noise due to the activity of the object (sample) itself. This activity may be due to variations in its many possible origins; for instance, variations due to biological reasons ("healthy" or "sick" tissues), increase or diminishing activity due to bruising, presence of pathogenes, enhance or inhibited blood flow [4], [5], [6], and many others. Therefore, the data available to analysis contains noise embedded which major part is due to the activity of sample itself (although, there is a very tiny part due to a random noise of setup, among others). The purpose of the Biospeckle is then to retrieve the underlying activity of the sample through the interference of light on it [7].

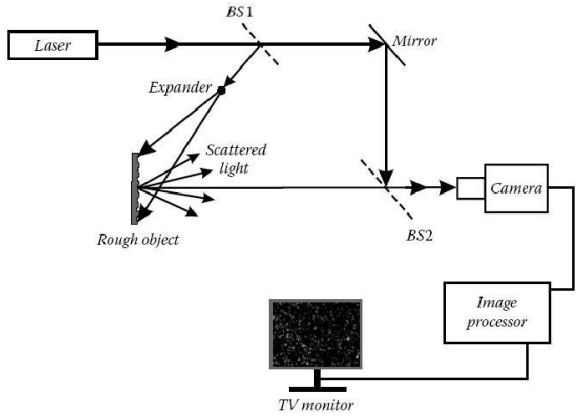

Figure 1. Schema of the experimental setup of an electronic speckle pattern interferometer. BS1 (BS2) represent regular Beamsplitters used to split (recombine) the laser beam before (after) the laser scattering on the sample. Through comparison of two beams we obtain the interference phenomena cause by the sample.

It is shown on Fig. 1 the experimental setup to acquire the image frames. It can be seen that the laser (monochromatic light) reflected on the mirror reaches the sample (object). The light is scattered by the sample (object) and it is acquired on CCD camera. The difference of laser optical path reflect by the sample produces the interference phenomena seen on the screen and showed on Fig. 2. This is the picture (frame) acquired on CCD camera at one specific time t_0. It is shown on Fig. 3 the evolution through time of a *subset* of the frame showed on Fig. 2. This *subset* is a given frame column of pixels whose activity is followed on time. In other words, the vertical axis corresponds to the pixel intensities of a given frame column of pixels at time t_0 and the following columns, along the horizontal axis, the pixel intensities of the same frame column of pixels along time.

It is visible on Fig. 3 the effect on time of the sample ac-

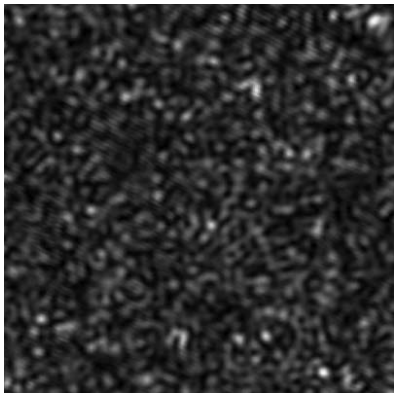

Figure 2. One frame of the video sequence.

tivity of the material. In the case of *high* activity (Fig. 3(a)), the speckle pattern is twinkling while in the case of *low* activity (Fig. 3(b)) the speckle pattern is more uniform and steady.

It is not the purpose of this work to introduce the Biospeckle technique, which has been studied and applied for at least a decade [8]. We focus on the statistical measurements for the Biospeckle analysis.

The activity of the sample (i.e., the Biospeckle) is technically achieved through a measure of the whole image along time called Generalized Difference (GD) [9], [10].

The Generalized Difference (GD) of a sequence of n integer values $s = [x_0, x_1, \ldots, x_{n-1}]$ is defined by Eq. 1.

$$GD(s) = \sum_{i=0}^{n-1} \sum_{j=i+1}^{n-1} |x_i - x_j| \tag{1}$$

When applied to the biospeckle, the sequence s is the sequence of values of one pixel along n frames of a video, as illustrated in Fig. 4. So we have one sequece s_p for each pixel p of the video.

The difference between the pixel intensities among all frames in the sequence is performed. The first summation regards the frame chosen as *reference* in the video sequence, while the second summation takes into account all the frames picked out after the chosen one. The cumulative value of differences evaluate above among all the *reference* frames chosen is the value of $GD(s)$ for the sequence (s) presented.

GD is presented on Fig. 5. Each pixel p of the image is the value $GD(s_p)$, where s_p is the sequence of the values $s_p = [x_0, x_1, \cdots, x_{n-1}]$ of the pixel intensities (x_i) of pixel p along time.

II. Fast computation of GD

In this section we introduce the steps to perform the evaluation of GD(s) (Eq. 1) faster than usually it is done. Firstly, we observe the module difference is evaluated only once for each pair of points in the sequence, as the second

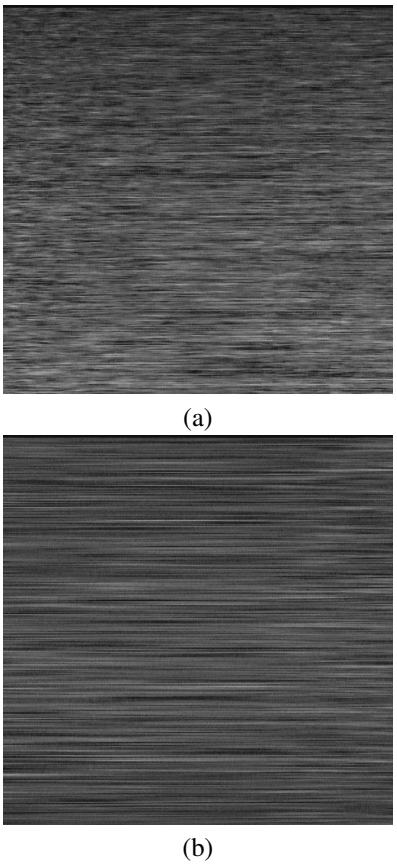

(a)

(b)

Figure 3. Temporal history of a speckle pattern of a material in high (a) and low (b) activity. Vertical line represents the activity of a specific vertical line in the frame, while the subsequent vertical lines show the evolution along time of this activity.

summation of the Eq. 1 begins at $j = i + 1$. Considering that

$$|x_i - x_j| = |x_j - x_i|$$

the GD(s) can also be defined as

$$GD(s) = \frac{1}{2} \sum_{i=0}^{n-1} \sum_{j=0}^{n-1} |x_i - x_j| \tag{2}$$

which can also be written as

$$GD(s) = \frac{1}{2} \left[\sum_{j=0}^{n-1} |x_0 - x_j| + \sum_{j=0}^{n-1} |x_1 - x_j| + \ldots \right.$$
$$\left. \ldots + \sum_{j=0}^{n-1} |x_{n-1} - x_j| \right] \tag{3}$$

Let us consider now that $x_i \in s$ be always a integer value belonging to the interval $[0 \ldots m-1]$. This set of values is

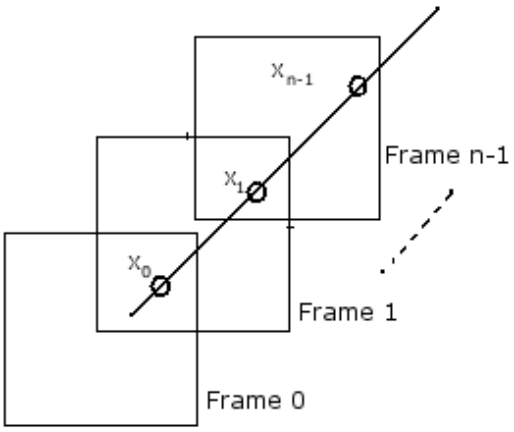

Figure 4. One pixel activity evolution. The activity of pixel p at frame $i(i = 0, 1, \cdots, n-1)$ is represented by x_i. The activity evolution of pixel p is thus represented by the sequence $s_p = [x_0, x_1, \ldots, x_{n-1}]$.

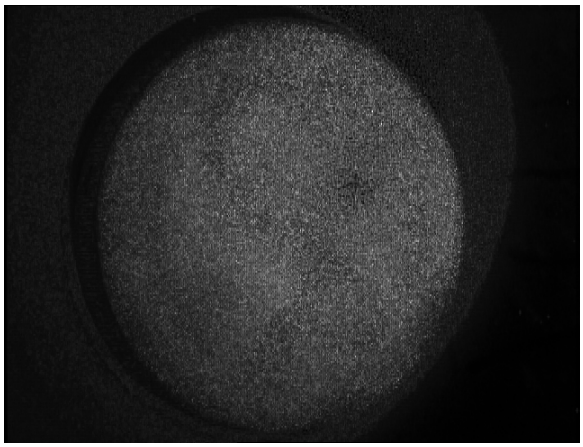

Figure 5. Generalized difference (GD). Each pixel p of the image is the value $GD(s_p)$, where s_p is the sequence of the values $s_p = [x_0, x_1, \cdots, x_{n-1}]$ of the pixel intensities (x_i) of pixel p along time.

typical in images analysis. In the case of Biospeckle, $m = 256$; i.e., gray levels.

Considering the integer values of the sequence s_p as the frame pixel intensities for a given pixel p in a video sequence of images, GD provides then a measure of the activity (on time) of the sample studied.

We propose a fast computation of GD(s), defined on Eq. 1 and expanded on Eq. 3, as follows.

The histogram of the sequence s on Eq. 3 is a sequence of $h(s) = [g_0, g_1, \ldots, g_{m-1}]$, where g_i is the number of occurrences of integer values of i in the sequence s [11].

Let us take the first summation of Eq. 3, which correspond to the term $i = 0$ of Eq. 2. This term can be rewritten as

$$\sum_{j=0}^{m-1} |x_0 - j| g_j$$

and therefore, we can rewrite Eq. 1 (expressed on the form of Eq. 2) as the form of Eq. 4 below

$$GD(s) = \frac{1}{2} \sum_{i=0}^{n-1} \sum_{j=0}^{m-1} |x_i - j| g_j \tag{4}$$

Now, we can also transform the first (outer) summation of Eq. 4 on the perspective of the histogram.

$$GD(s) = \frac{1}{2} \sum_{i=0}^{m-1} \left(\sum_{j=0}^{m-1} |i - j| g_j \right) g_i$$

or

$$GD(s) = \sum_{i=0}^{m-1} \left(\sum_{j=i+1}^{m-1} |i - j| g_j \right) g_i$$

Let us consider

$$P_i = \sum_{j=i+1}^{m-1} |i - j| g_j$$

We then have

$$GD(s) = \sum_{i=0}^{m-1} P_i g_i \tag{5}$$

Note that

$$\begin{aligned} P_0 &= g_1 + 2g_2 + 3g_3 + \ldots + (m-1)g_{m-1} \\ P_1 &= g_2 + 2g_3 + 3g_4 + \ldots + (m-2)g_{m-1} \\ P_2 &= g_3 + 2g_4 + 3g_5 + \ldots + (m-3)g_{m-1} \end{aligned}$$

Therefore,

$$\begin{aligned} P_1 &= P_0 - [g_1 + g_2 + \ldots + g_{m-1}] \\ P_2 &= P_1 - [g_2 + g_3 + \ldots + g_{m-1}] \end{aligned}$$

In other words,

$$\begin{aligned} P_1 &= P_0 - \sum_{j=1}^{m-1} g_j \\ P_2 &= P_1 - \sum_{j=2}^{m-1} g_j \end{aligned}$$

If we consider

$$S_i = \sum_{j=i}^{m-1} g_j$$

We can observe that

$$P_{i+1} = P_i - S_{i+1}$$

Note that

$$S_0 = \sum_{j=0}^{m-1} g_j = n$$

where n is the total number of elements in the sequence (Eq. 1), which in Biospeckle analysis corresponds to the number of frames in the video sequence.

Note also that

$$S_{i+1} = \sum_{j=i+1}^{m-1} g_j = S_i - g_i$$

If we consider that GD has been already evaluate for the first k values of i on Eq. 5, we have

$$GD_k(s) = \sum_{i=0}^{k} P_i g_i$$

In order to evaluate GD for the first $k+1$ values of i, we have

$$GD_{k+1}(s) = GD_k(s) + P_{k+1} g_{k+1}$$

Therefore, we have a **mathematical induction** described as:

(i) initial condition:

$$\begin{aligned} S_0 &= n \\ P_0 &= \sum_{j=1}^{m-1} j g_j \\ GD_0(s) &= P_0 g_0 \end{aligned}$$

(ii) inductive step:

$$\begin{aligned} S_{k+1} &= S_k - g_k \\ P_{k+1} &= P_k - S_{k+1} \\ GD_{k+1}(s) &= GD_k(s) + P_{k+1} g_{k+1} \end{aligned}$$

(iii) stop condition:

$$k = m - 1$$

The stop condition (step (iii)) comes from the fact that $GD_{m-1}(s) = GD(s)$.

Finally, we can rewrite an algorithm to evaluate GD in time $O(n)$, for $n > m$, or $O(m)$, for $m > n$. The time $O(n)$ is the time to evaluate the histogram. The time $O(m)$ is the evaluation time of P_0 on inicialization and also is the execution time of m inductive steps.

III. Alternative generalized difference GD^*

In this section we present an alternative measurement that we call GD^*.

The absolute value in Eq. 1 has been used to guarantee that all the terms of the sum are positive. It is usual the use of the squared value in place of the absolute value, since the function $f(x) = |x|$ has the same order as the function $g(x) = x^2$. Say,

$$f(x') > f(x) \Leftrightarrow g(x') > g(x) \tag{6}$$

So we propose to replace the absolute values in Eq. 1 by squared values. Due the similarity between squares and absolute values, the resultant equation is an alternative generalized difference measurement. Denote by GD^*, it is defined by

$$GD^*(s) = \sum_{i=0}^{n-1} \sum_{j=i+1}^{n-1} (x_i - x_j)^2 \tag{7}$$

The GD^* is presented in Fig. 6. As well as in Fig. 5, each pixel p of Fig. 6 is the value $GD(s_p)$, in (a), or $GD^*(s_p)$, in (b), where s_p is the sequence of the values of the pixel p along time.

Notice that the main difference between Fig. 6(a) and Fig. 6(b) is the contrast. There is a more visible contrast in Fig. 6(b), due to the higher values obtained by the application of squares in place of absolute values. However, in both images it is possible to observe the contour of the character in the coin, and also the high activity over the coin, where ink has been applied.

It is important to emphasize that the GD^* is an alternative measurement. There is no direct relationship between GD and GD^*. As stated before, there is a similarity between squares and absolute values in terms of Eq. 6, which as an order relationship. The order relationship, however, does not hold for sums of squares and sums of absolute values, so it does not hold for GD^* and GD. A counter-example is easy to be found. Let $s = [1, 1, 10]$ and $s' = [1, 3, 11]$, we have

$$\begin{aligned} GD(s) &= |1-1| + |1-10| + |1-10| = 18 \\ GD(s') &= |1-3| + |1-11| + |3-11| = 20 \\ GD^*(s) &= (1-1)^2 + (1-10)^2 + (1-10)^2 = 192 \\ GD^*(s') &= (1-3)^2 + (1-11)^2 + (3-10)^2 = 168 \end{aligned}$$

Observe that $GD(s') > GD(s)$ does not imply $GD^*(s') > GD^*(s)$.

Having shown the above remarks, we show in the next section that GD^* has a straight relationship with the variance.

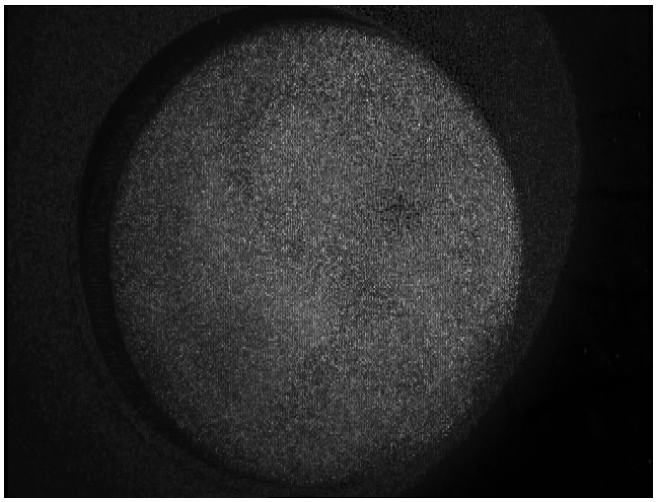

(a)

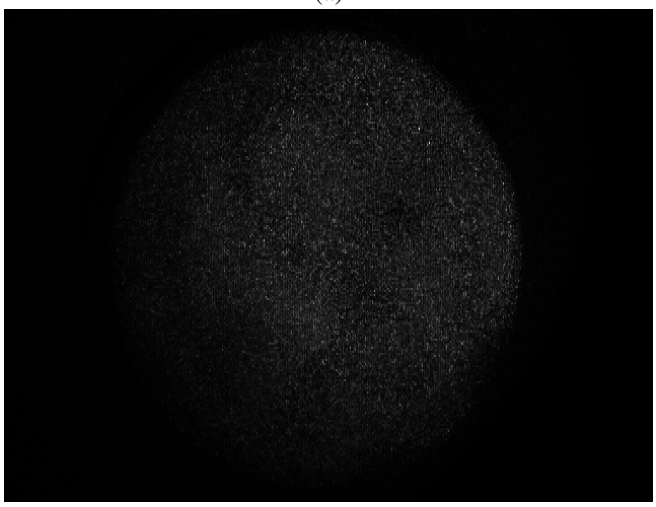

(b)

Figure 6. Comparison between GD and GD^*. The GD is in (a), and GD^* is in (b). Each pixel p is the value $GD(s_p)$, in (a), or $GD^*(s_p)$, in (b), where s_p is the sequence of the values of the pixel p along time.

IV. The GD^* as a function of the variance

The direct implementation of the GD^* would be the brute force double sum, which is clearly $\mathcal{O}(n^2)$. In this section we develop Eq. 7 and we show that GD^* is a function of the variance, so it can be computed in $\mathcal{O}(n)$.

Since

$$(x_i - x_j)^2 = (x_j - x_i)^2$$

We can rewrite Eq. 7 to obtain

$$GD^*(s) = \frac{1}{2}\sum_{i=0}^{n-1}\sum_{j=0}^{n-1}(x_i - x_j)^2 \tag{8}$$

And so expand it to

$$GD^*(s) = \frac{1}{2}\sum_{i=0}^{n-1}\sum_{j=0}^{n-1} x_i^2 - 2x_i x_j + x_j^2$$

compute the sum on j

$$\begin{aligned} GD^*(s) &= \frac{1}{2}\sum_{i=0}^{n-1} nx_i^2 - 2x_i(n\overline{x}) + n\overline{x^2} \\ &= \frac{1}{2}\sum_{i=0}^{n-1} nx_i^2 - 2nx_i\overline{x} + n\overline{x^2} \end{aligned}$$

compute the sum on i

$$\begin{aligned} GD^*(s) &= \frac{1}{2}\left(n(n\overline{x^2}) - 2n(n\overline{x})\overline{x} + n(n\overline{x^2})\right) \\ &= \frac{1}{2}\left(n^2\overline{x^2} - 2n^2\overline{x}^2 + n^2\overline{x^2}\right) \\ &= \frac{1}{2}\left(2n^2\overline{x^2} - 2n^2\overline{x}^2\right) \end{aligned}$$

and finally obtain

$$GD^*(s) = n^2(\overline{x^2} - \overline{x}^2) \tag{9}$$

Equation 9 shows that the GD^* is a function of the variance. Remember that the variance, defined by

$$\sigma^2(s) = \frac{1}{n}\sum_{i=0}^{n-1}(x_i - \overline{x})^2$$

can also be rewritten. We first expand it to

$$\sigma^2(s) = \frac{1}{n}\sum_{i=0}^{n-1}(x_i^2 - 2x_i\overline{x} + \overline{x}^2)$$

compute the sum on i

$$\sigma^2(s) = \frac{1}{n}\left(n\overline{x^2} - 2n\overline{x}^2 + n\overline{x}^2\right)$$

and finally obtain

$$\sigma^2(s) = \overline{x^2} - \overline{x}^2 \tag{10}$$

By joining Eqs. 9 and 10, we see that

$$GD^*(s) = n^2\sigma^2(s) \tag{11}$$

Since the variance (Eq. 10) can be computed in $\mathcal{O}(n)$, the GD^* can also be computed in $\mathcal{O}(n)$.

It is useless to show a visual comparison (such as Fig. 6) between the variance and the GD^*, because both images are equal if the gray scale is normalized.

Indeed, by the results of this section we can observe that the GD^* is equivalent to the variance.

V. Discussion

In this paper we have shown different viewpoints for generalized differences. We have analyzed the most popular measurement: the GD.

First, we have pointed that the GD computation is implemented by the direct brute force algorithm, which is $\mathcal{O}(n^2)$, and then we have provided and proved an alternative algorithm for it. The alternative algorithm has an asymptotic complexity $\mathcal{O}(n)$ due to a change on the computation paradigm. The proposed algorithm is computed on the histogram of the sequence, and not on the sequence itself.

Second, we have questioned the use of absolute values in the equation of the GD (Eq. 1), and we have proposed the GD^*, that uses squared values in place of absolute values. We have pointed that the GD and the GD^* are not equivalent, but they have qualitative similarities that allows us to replace one by the other in many applications.

Third, we have shown that the GD^* is a function of the variance. The introduction of the GD^* equation has been necessary only to help us conclude that there are qualitative similarities between the GD and the variance.

The GD and the variance are global measurements. Both measurements consider each pixel as a random variable, and the values of the pixel along time as a non ordered set of observations. This procedure generates thus a loss of the temporal information.

Since the Biospeckle technique is used to study the activity of a material, and the study is performed by observing temporal variations on fixed points, the loss of temporal order produced by the GD means that this measure cannot be used by itself. In addition of temporal order loss, there is a issue regarding normality. The analysis of variances is usually applied to a sample of observations that have been drawn from a normal distribution. When applied to a non-normal distribution, the variance analysis can only show how much the data is spread around the average, but it cannot show how it is spread. It means that one cannot conclude anything about the behavior of the pixel intensity activity along time. Since we cannot assume that the material activity follows a normal distribution, the variance analysis, by itself, has limitations. As a consequence, the GD has limitations too. Although useful, it is recommended to use complementary measures.

To sustain the above statement, we compare the GD with a measurement that takes on account temporal variation. Such measurement has been recently defined by our research team, and it has not yet been widely adopted by the Biospeckle community due to its recent proposal. Let us call it WD, which is defined by

$$WD(w,s) = \sum_{i=0}^{n-1} \sum_{j=i+1}^{i+w} |x_i - x_j| \qquad (12)$$

where w is the size of the time window. Notice that the internal sum is performed only on the w observations subsequent to observation i. This means that the WD is a sum of variations *along local time windows*.

We show a comparison between GD and WD in Fig. 7.

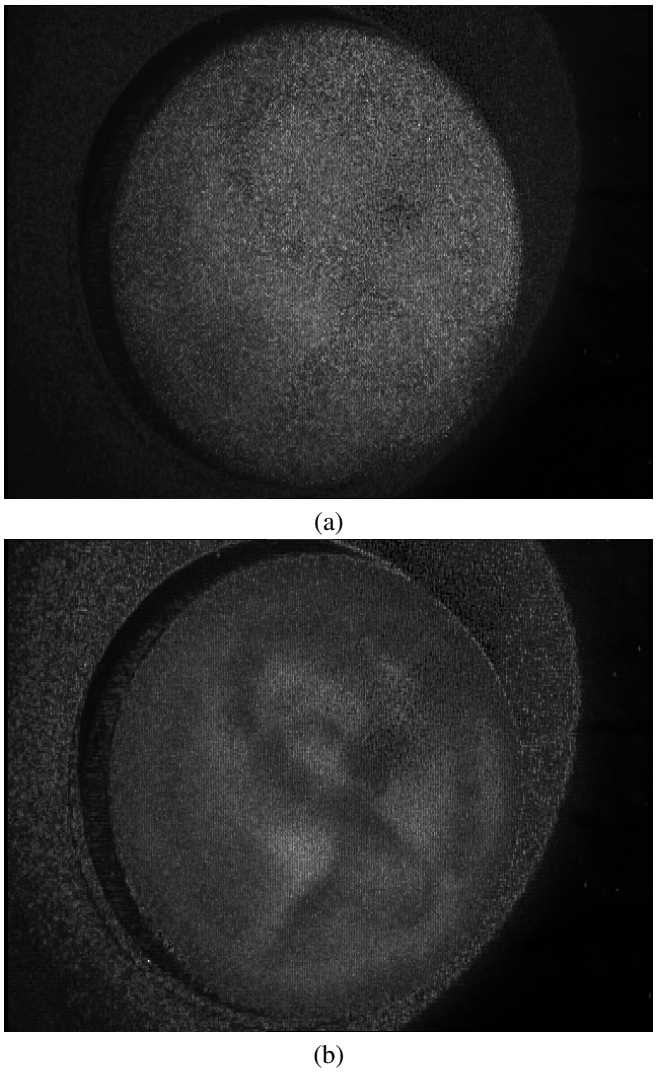

(a)

(b)

Figure 7. Comparison between GD and WD for $w = 5$. The GD is in (a), and WD is in (b). Each pixel p is the value $GD(s_p)$, in (a), or $WD(w, s_p)$, in (b), where s_p is the sequence of the values of the pixel p along time.

The results in this case are visually very different. The WD allows us to better observe the silhouette printed on the coin. One can suppose that the ink over the silhouette's border has dried faster than the ink over other regions, since the dry ink does not present activity.

Finally, we alert that although the GD is the most popular measurement used for Biospeckle analysis, this measurement has limitations, and it should not be the only measurement applied in any application. It is recommended to apply also some measurements that are able to observe variations

in local time windows like the WD. In an extended version of this paper we will provide a detailed analysis of the WD.

VI. Conclusion and future work

In this paper we have presented qualitative similarities between the GD and the variance. We have stated that the data obtained by the image acquisition step of the Biospeckle technique is an observation of the activity of the material in study, and we cannot expect that the activity on a fixed point of the material should be drawn from a normal distribution. Since the analysis of variances is usually applied to normal distributions, and the GD is qualitatively similar to the variance, we conclude that the GD has limitations, and it cannot be the only measurement used in analysis of Biospeckle.

Finally, we have stated that other measurements applied to Biospeckle data, in addition to the GD, should be measurements of variations on local time windows, such as the WD presented in Section V.

In an extended version of this paper we will exploit qualitatively and quantitatively the measurements of variations on local time windows. We will show the relationship of the WD with known signal processing filters, and we will present variations of the WD based on such relationship. We will also analyze a third measurement method presented in [3], [12], the Fujii's method which has yet another physical meaning [13], [14].

Acknowledgment

The authors would like to thank Fapemig and CNPq for the financial support.

References

[1] J. W. . Goodman, "Some fundamental properties of speckle," *Journal of Optical Society of America*, vol. 66, p. 1145, 1976.

[2] J. W. Goodman, *Laser Speckle and Related Phenomena*, 2nd ed. New York: Springer Verlag, 1984, ch. Statistical properties of laser speckle patterns.

[3] H. J. Rabal and R. A. B. Jr., Eds., *Dynamic laser speckle and applications*. CRC Press, Nov. 2009.

[4] A. Dunn, A. Devor, H. Bolay, M. Andermann, M. Moskowicz, A. Dale, and D. Boas, "Simultaneous imaging of total cerebral hemoglobin concentration, oxygenation , and blood flow during functional activation," *Optical Letters*, vol. 28, p. 28, 2003.

[5] H. Rabal, N. Cap, M. Trivi, R. Arizaga, A. Federico, G. E. Galizzi, and G. H. Kaufmann, "Speckle activity images based on the spatial variance of the phase," *Applied Optics*, vol. 45, no. 34, pp. 8733–8, 2006.

[6] S. E. Murialdo, G. H. Sendra, I. P. Luca, R. Arizaga, J. F. Gonzalez, H. Rabal, and M. Trivi, "Analysis of bacterial chemotactic response using dynamic laser speckle," *Journal of Biomedical Optics*, vol. 14, no. 6, 2009.

[7] J. W. Goodman, *Speckle Phenomena in Optics: Theory and Applications*. Roberts & Company, 2007.

[8] J. A. Wardell, K and G. Nilsson, "Laser perfusion imaging by dynamic light scattering," *IEEE Trans. Biomed. Eng.*, vol. 40, no. 4, p. 309, 1993.

[9] R. Arizaga, N. Cap, H. Rabal, and M. Trivi, "Display of the local activity using dynamical speckle patterns," *Optical Engineering*, vol. 41, p. 287, 2002.

[10] G. Romero, E. Alans, and H. Rabal, "Statistics of the dynamic speckle produced by a rotating diffuser and its application to the assessment of paint drying," *Optical Engineering*, vol. 39, no. 6, p. 1652, 2000.

[11] R. C. Gonzalez and R. E. Woods, *Digital image processing*, 2nd ed. Prentice Hall, 2002.

[12] H. J. Rabal, *Dynamic laser speckle and applications*. CRC Press, 2009, ch. Activity images, pp. 115–136.

[13] H. Fujii, T. Asakura, K. Nohira, Y. Shintomi, and T. Ohura, "Blood flow observed by time-varying laser speckle," *Optical Letters*, vol. 10, no. 3, p. 104, 1985.

[14] H. Fujii, K. Nohira, Y. Yamamoto, H. Ikawa, and T. Ohura, "Evaluation of blood flood by laser speckle image sensing part 1," *Applied Optics*, vol. 25, no. 24, p. 5321, 1987.